Fe(III) Complexed Polydopamine Modified Mg/Al Layered Double Hydroxide Enhances The Removal of Cr(VI) From Aqueous Solutions

Changcheng Chen
Southwest Petroleum University
Mina Luo (luo_mn@126.com)
Southwest Petroleum University
Fu Chen
Southwest Petroleum University
Chao Huang
Southwest Petroleum University
Chunmei Zhu
Southwest Petroleum University
Hongjun Wu
Petrochina Tarim Oilfield Co

Research Article

Keywords: Composite material, Polydopamine, Layered double hydroxides, Adsorption, Cr(VI)

Posted Date: September 7th, 2021

DOI: https://doi.org/10.21203/rs.3.rs-854606/v1

Version of Record: A version of this preprint was published at Journal of Polymers and the Environment on January 17th, 2022. See the published version at https://doi.org/10.1007/s10924-022-02375-8.

Fe(III) complexed polydopamine modified Mg/Al layered double hydroxide enhances the removal of Cr(VI) from aqueous solutions

Changcheng Chen[a], Mina Luo[a,] *, Fu Chen[a], Chao Huang[a], Chunmei Zhu[a], Hongjun Wu[b]

[a] College of Chemistry and Chemical Engineering, Southwest Petroleum University, Chengdu, China;
[b] Research Institutes of Petroleum Engineering, PetroChina Tarim Oilfield Company, Korla, China

ABSTRACT

Herein, we report the preparation of Fe(III) complexed polydopamine modified Mg/Al layered double hydroxides composite material (LDHs@PDA-Fe(III)) and its application to the removal of Cr(VI) in aqueous solution. LDHs@PDA-Fe(III) was characterized and analyzed by field-emission scanning electron microscopy-energy dispersive X-ray spectroscopy (SEM-EDS), Fourier transformed infrared (FTIR), X-ray diffraction (XRD), X-ray photoelectron (XPS). The adsorption performance was studied through a series of adsorption experiments. Under the influence of pH, time, temperature, concentration, the maximum adsorption capacity obtained in the experiment is 683.4 mg/g. In addition, after 5 adsorption cycles, LDHs@PDA-Fe(III) still shows excellent adsorption capacity and stability. Combining adsorption experiments and characterization analysis, it is inferred that the adsorption of Cr(VI) by LDHs@PDA-Fe(III) is the result of the synergistic effect of multiple adsorption mechanisms. Therefore, the efficient removal capacity and excellent stability make LDHs@PDA-Fe(III) an ideal adsorbent for removing Cr(VI) from aqueous solutions.

* Corresponding author.
E-mail address: luo_mn@126.com (M. Luo).

KEYWORDS: Composite material, Polydopamine, Layered double hydroxides, Adsorption, Cr(VI)

1. Introduction

Hexavalent chromium (Cr(VI)) is a common heavy metal pollution because of extensive use and emission in industrial activities. Compared with another oxidation states of trivalent chromate (Cr(III)), Cr(VI) poses a greater threat to the ecosystem due to its teratogenesis and cancerogenic [1][2]. The World Health Organization (WHO) stipulates that the maximum concentration of Cr (VI) in surface water and drinking water cannot exceed 0.1 and 0.05 mg/L, respectively [3]. Up to now, many methods have been developed and applied to separate Cr(VI) from aqueous medium through the physical and chemical processes, such as photocatalytic reduction [4], ion exchange [5], membrane separation [6], and adsorption [7]. Compared to other methods, adsorption is a promising technique for remediation of Cr (VI) contamination in water because of its low cost and easy operation [8][9]. Currently, A variety of adsorbents are used for Cr (VI) removal from aqueous solutions, involving double hydroxide composites [10][11], biochar [12][13], metal-organic framework [14][15], zeolite [16], and zero-valent iron [17]. However, Disadvantages such as low efficiency still limit their widespread use. Therefore, it is necessary to solve these problems through the research of novel adsorbents.

Recently, organic-inorganic hybrid materials have attracted wide attention because of their good adsorption capacity and multifunctional groups [18]. Layered double hydroxides (LDHs) is a kind of layered material with the general molecular formula of $[M_{1-x}^{2+}M_x^{3+}(OH)_2]^{x+}(A^{n-})_{x/n}\cdot mH_2O$, where M^{2+} and M^{3+} represented divalent and trivalent metal cations in the positively charged host layers respectively, and A^{n-} represented interlayer anion. LDHs contains a large number of exchangeable interlayer anions, which has an advantage excellent anion removal ability. LDHs has been widely used in the remediation of wastewater contaminated by heavy metal ions. For example, Mg/Al LDHs intercalated biochar was obtained by in-situ calcination, and it has high Cr (VI) removal ability [19]; A ternary core-shell adsorbent based on the in-situ growth of Mg/Al LDHs on polyaniline-coated biochar was successfully synthesized and used for the removal of diclofenac in water,

showing excellent adsorption capacity [20], Therefore, LDHs has become a promising anion adsorbent for the removal of anion pollutants in water due to its efficient anion exchange ability [21][22].

Polydopamine (PDA) has been widely used as a modified material because of its ability to oxidize and self-polymerize under alkaline conditions and attach to the surface of various materials [23][24][25], Moreover, it is worth noting that PDA contains a large number of hydroxyl and amino functional groups which could act as the cloning sites of Cr(VI) [26][27]. However, due to the interaction between covalent and non-covalent dopamine (DA) molecules in the polymerization process, the PDA coating will be adversely affected, resulting in the uneven deposition on the surface of the material [28]. Recent studies have found that PDA can form coordination bonds with a variety of transition metal metals, such as copper ions [29], titanium oxides [30], and iron ions [31]. The mussel, for example, improves the rigidity and elongation of its threads by binding iron ions (Fe(III)) tightly to the catecholin-like side chains of the 3,4-dihydroxyphenylalanine (DOPA) [32]. By first forming complexes with DA, Fe(III) can also accelerate the polymerization process of DA to form a more uniform and dense PDA deposit [33]. The Fe(III) chelated in PDA can also provide new binding sites for pollutants to enhance their adsorption capacity [34].

In this work, Fe(III) was chelated into PDA network and quickly deposited on the surface of Mg/Al LDHs under alkaline conditions. A novel nano-adsorbent named LDHs@PDA-Fe(III) was prepared. The adsorption properties were systematically studied by batch adsorption experiments. Regeneration experiments were also carried out to assess the possibility of sustainable application and the stability of the adsorbent. In addition, the potential adsorption mechanism was studied by different characterization techniques.

2. Materials and methods

2.1 Materials

$Mg(NO_3)_2 \cdot 6H_2O$, $Al(NO_3)_3 \cdot 9H_2O$, hexamethylene tetramine (HMT), dopamine hydrochloride, tris (hydroxymethy) aminomethane (Tris), $FeCl_3 \cdot 6H_2O$ were bought

from Chengdu Chron Chemicals Co. Ltd. Cr(VI) stock solution is obtained by dissolving $K_2Cr_2O_7$ in deionized water. All the chemicals used in the experiments were analytically pure and without any further purification.

2.2 Preparation of Mg/Al LDHs

Mg/Al LDHs were synthesized by a simple method [35]. 7.8 mmol $Mg(NO_3)_2 \cdot 6H_2O$, 2.6mmol $Al(NO_3)_3 \cdot 9H_2O$ and 9.2 mmol HMT were accurately dissolved in 40 mL deionized water and stirred at high speed for 30min at room temperature. Then it was transferred into a high-pressure reaction kettle lined with built-in PTFE, and reacted at 140℃ for 12h. After the sample was cooled to room temperature, it was filtered and separated, rinsed with deionized water for three times and dried at 70℃ for 12h.

2.3 Preparation of LDHs@PDA-Fe(III)

The preparation process of polydopamine doped Fe(III) modified Mg/Al layered dihydroxide is shown in Fig. 1. 0.2 g LDHs is dispersed in 100 mL deionized water. Then 0.121 g trimethylaminomethane (10mol/L), 0.4 g dopamine hydrochloride and 0.1425 g $FeCl_3 \cdot 6H_2O$ were added successively. The pH of the solution was adjusted to 8.5 with 1mol/L NaOH, and the reaction was stirred at room temperature for 24 h. The products were filtered and collected, and rinsed with deionized water for three times. After drying at 70℃ for 12 h, polydopamine modified Mg/Al layered dihydroxide LDHs@PDA without $FeCl_3 \cdot 6H_2O$ was prepared by the same method.

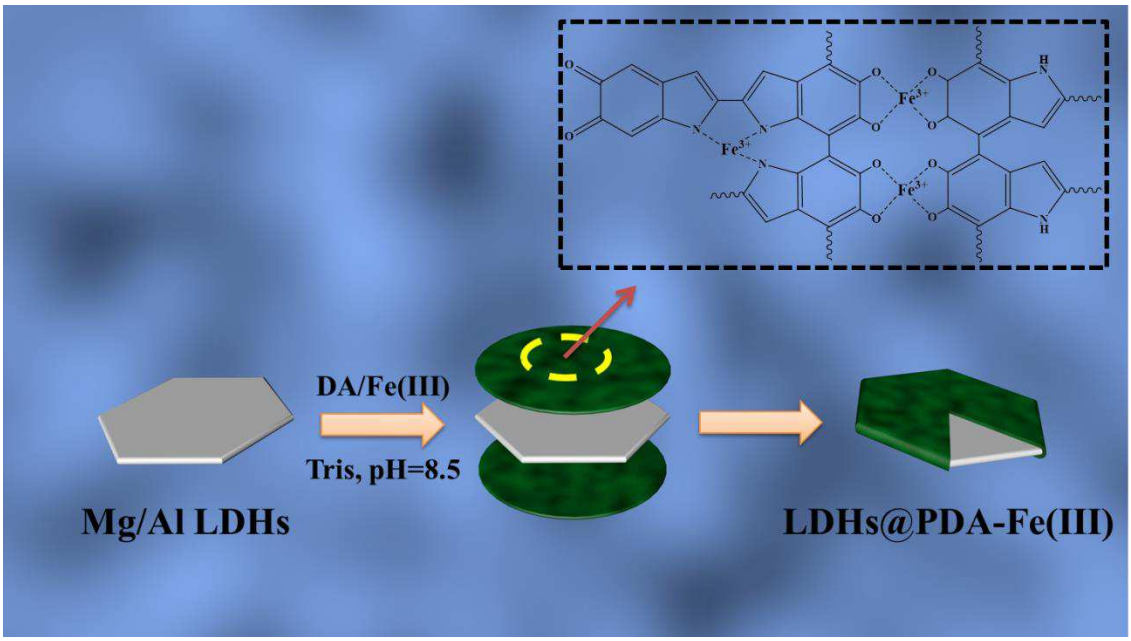

Fig. 1 synthetic process for the LDHs@PDA-Fe(III).

2.4 Adsorption experiments

All batch adsorption experiments were performed by adding 20 mg of adsorbent to 50 mL Cr(VI) solution. After an oscillating adsorption at 298 K with 160rpm for a specified time, the adsorbent and solution were separated by a 0.45 μm filter (nylon) and the remaining Cr(VI) concentration was measured by a visible light spectrophotometer (V-1800) at 540 nm. The effect of pH was evaluated in increments of one pH unit between pH 3.0 to 9.0. The influence of Cr(VI) initial concentration was studied by controlling the initial concentration of Cr(VI) from 80 to 800 mg/L. The adsorption kinetics was experimentally studied in the adsorption time range from 10 to 540 min. The adsorption isotherm experiment was carried out by setting the initial concentration of Cr(VI) from 80-800 mg/L at 298, 313 and 328 K. The adsorption capacity of Cr(VI) was calculated by Eq. (1):

$$q_t = \frac{(C_t - C_0)*V}{m} \quad (1)$$

Where C_0 (mg/L), C_t (mg/L) are the concentration of Cr(VI) at the initial time and t time; V (L) is the volume of Cr(VI) solution; m (mg) represents the amount of adsorbent added; q_t (mg/g) is the adsorption capacity of Cr(VI) at time t.

The desorption experiment was carried out as follows. The initial concentration

of Cr(VI) was 100 mg/L, the solution pH was 3, and the adsorbent dose was 20mg. After adsorption at room temperature for 24 hours, residual Cr(VI) concentration was determined. After centrifugation, the adsorbent was desorbed with 0.05M NaOH for 24h and washed with deionized water for several times. After drying overnight at 70℃, the spent- LDHs@PDA-Fe(III) was used to repeat the desorption-regeneration cycles 5 times under same conditions to assess the reusable performance of LDHs@PDA-Fe(III).

3. Result and discussion

3.1 Characterization of materials

The micro-morphology differences of LDHs, LDHs@PDA, LDHs@PDA-Fe(III) and LDHs@PDA-Fe (III) after adsorption are shown in Fig. 2. It can be seen from Fig. 2a that Mg/Al LDHs are successfully synthesized with a size of about 1-2μm. As shown in Fig. 2b, after PDA modification, the surface of LDHs@PDA is more rounded and a large number of PDA particles are present, which may be caused by the uneven and non-dense deposition of PDA. As shown in Fig. 2c, after Fe(III) is added, the rounded and granular feeling of the surface of LDHs@PDA-Fe (III) is significantly reduced. This indicates that the PDA distribution on the surface is more uniform and compact [33], and there is no significant difference in LDHs@PDA-Fe(III) before and after adsorption, indicating that the material is relatively stable in the adsorption process. EDS spectra of LDHs@PDA-Fe(III) before and after adsorption are shown in Fig. 3. There are a large number of C, O and other elements on the surface of LDHs@PDA-Fe (III) and a large number of Fe elements are also detected, indicating that Fe(III) is successfully fixed on the surface of the material. After adsorption, a large number of Cr(VI) elements were newly detected, indicating that Cr(VI) was successfully adsorbed and fixed on the surface of the material.

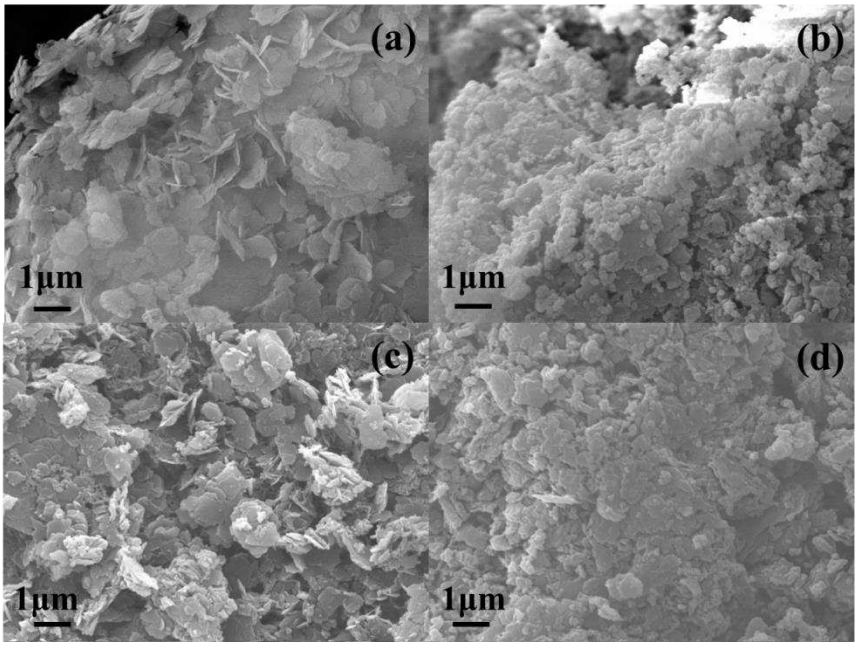

Fig. 2 SEM images of (a) LDHs, (b) LDHs@PDA, (c) LDHs@PDA-Fe(III) and (d) LDHs@PDA-Fe (III) after adsorption.

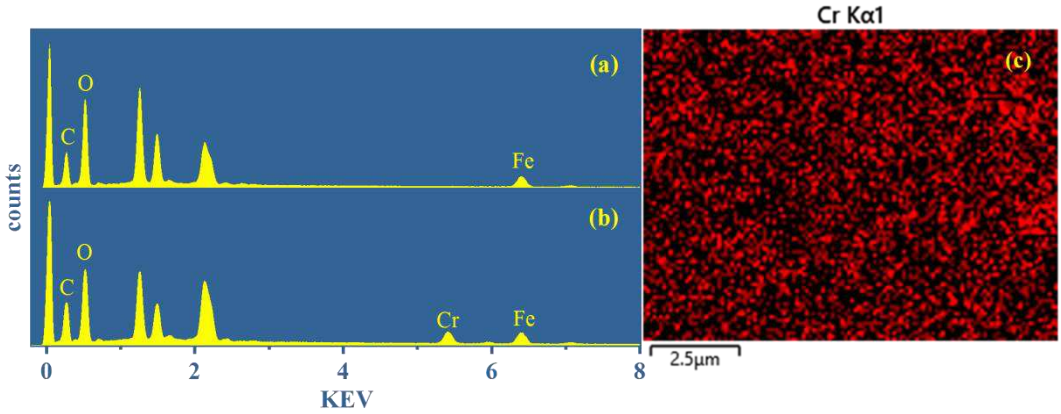

Fig. 3 EDS spectra of (a) LDHs@PDA-Fe(III) and (b) LDHs@PDA-Fe (III) after adsorption and (c) Cr distribution onto LDHs@PDA-Fe (III) after adsorption.

FT-IR analysis results of LDHs, LDHs@PDA and LDHs@PDA-Fe (III) are shown in Fig. 4a. Among them, the peaks at 446 cm^{-1}, 551 cm^{-1}, 679 cm^{-1} and 782 cm^{-1} are lattice vibration of M-O, O-M-O and M-O-M (M = Mg and Al) in LDHs[35]. The strong absorption at 3446 cm^{-1} and 1628 cm^{-1} correspond to the stretching vibration of OH and C=O respectively [36], and the peaks at 1356 cm^{-1} are related to CO_3^{2-} in LDHs. After modified by PDA [37], new band of LDHs@PDA appeared at 1483 cm^{-1}, 1420 cm^{-1} and 1281 cm^{-1}, which were derived from the stretching vibration of aromatic ring in PDA, the shear vibration of N-H in PDA layer and the stretching vibration peak of C-O in C-O-H, respectively. In addition, the new band of

LDHs@PDA-Fe(III) at 580 cm^{-1} belongs to the stretching vibration absorption peak of Fe-O [33]. The above results indicate that, compared with LDHS, the PDA-modified LDHs@PDA has a large number of additional functional groups that can be used as Cr(VI) adsorption sites. In addition, the infrared results of LDHs@PDA-Fe(III) indicate that the doped Fe(III) may be fixed in the form of Fe-O [33][38].

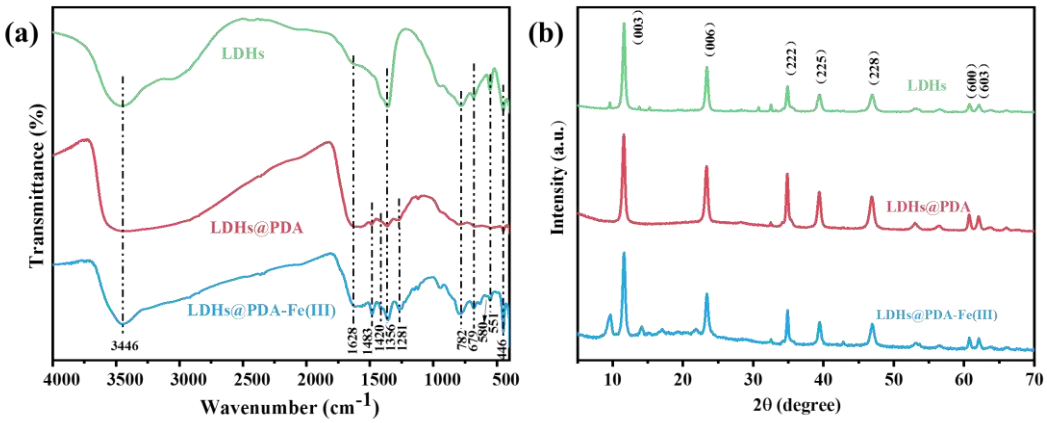

Fig. 4 (a) FT-IR spectra of LDHs, LDHs@PDA and LDHs@PDA-Fe(III); (b) XRD spectra of LDHs, LDHs@PDA and LDHs@PDA-Fe(III).

In order to study the existence forms of crystals in LDHs, LDHs@PDA and LDHs@PDA-Fe(III), XRD was used for characterization analysis. The results are shown in Fig 4b. The strong diffraction peak of three materials at 2θ=11.68° (003), 23.52° (006), 34.88° (222), 39.47° (225), 46.99° (228), 60.72° (600) and 62.11° (603) are attributed to the characteristic of Mg/Al LDHs nanoplates (JCPDS card 51-1525) [22]. In addition, the XRD peaks of the three materials are not significantly different. The diffraction peaks of other impurities are not detected, indicating that Mg/Al LDHs is the only crystal in the material, and has excellent stability and high purity, and the diffraction peaks of the three materials are all sharp and symmetrical, wich indicates that the highly crystallinity of Mg/Al LDHs [35].

3.2 Effect of pH

The pH value of the system can not only affect the existing form of Cr(VI) in solution, but also affect the surface charge property of the adsorbent material, which could affect the electrostatic force between the adsorbent and Cr(VI). The effects of pH are demonstrated in Fig. 5a. Under the same conditions, the adsorption capacity of

LDHs, LDHs@PDA and LDHs@PDA-Fe(III) decreases gradually with the increase of pH. The adsorption capacity of LDHs@PDA-Fe(III) is better than that of LDHs@PDA and LDHs in the whole pH range. The adsorption capacity of these three materials were 210.2 mg/g, 109.4 mg/g and 61.1 mg/g, respectively, when pH of solution reaches 3.0. When pH=9, compared with the adsorption data at pH=3, the adsorption capacity of Cr(VI) by these three materials decreased by 78.3%, 81.8% and 96%, respectively. In combination with the Zeta potential data of LDHs@PDA-Fe(III) (Fig. 5b), it is speculated that when the pH < 5.6, the LDHs@PDA-Fe(III) is positively charged due to the protonation of surface functional groups [39]. At the same time Cr(VI) in the solution exists in the form of anions. The electrostatic force between LDHs@PDA-Fe(III) and Cr(VI) is electrostatic attraction. Wich increases with the decrease of pH. On the contrary, when the system pH>5.6, LDHs@PDA-Fe(III) is negatively charged due to the deprotonation of surface functional groups. And the electrostatic repulsive force could impede the adsorption process of Cr(VI) by LDHs@PDA-Fe(III). In addition, there may be competing adsorption between OH^- and Cr(VI) in the system [40]. With the increase of pH, the content of OH^- in the system gradually increases, which intensifies the competitive adsorption behavior between OH^- and Cr(VI) [41], thus reducing the adsorption amount of Cr(VI).

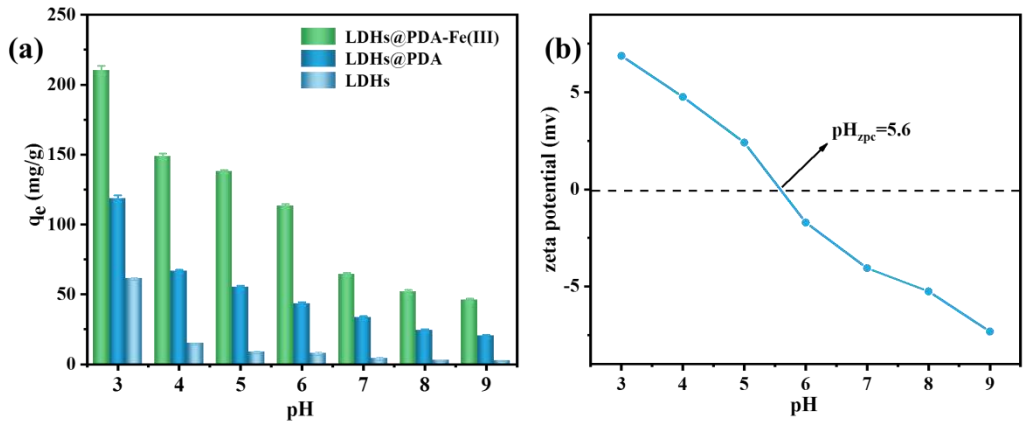

Fig. 5 (a) effect of pH on Cr(VI) adsorption by LDHs, LDHs@PDA and LDHs@PDA-Fe(III) at concentration of 100 mg/L, T=298 K, m=20 mg; (b) the zeta-potential of LDHs@PDA-Fe(III) as a function of pH.

3.4 Adsorption kinetics

Pseudo-first-order and pseudo-second-order kinetic models were used to fit the adsorption data of LDHs@PDA-Fe(III) and LDHs@PDA adsorption, respectively. Their model expressions were as follows:

Pseudo-first-order： $q_t = q_e(1-e^{-k_1 t})$ (2)

Pseudo-second-order： $q_t = \frac{q_e^2 k_2 t}{1+k_2 q_e t}$ (3)

Where t (min) is adsorption time; q_t (mg/g) and q_e (mg/g) represent the adsorption capacity of Cr(VI) at time t and the adsorption capacity at equilibrium respectively; k_1 (min^{-1})and k_2 ($g \cdot mg^{-1} \cdot min^{-1}$) represent the kinetic rate constant. The results are shown in Fig. 6 and Table 1 and Table 2. These two materials showed similar adsorption behavior for Cr(VI), and the adsorption rate decreased rapidly with the increase of time. At 60 min, the adsorption capacity of LDHs@PDA-Fe(III) and LDHs@PDA reached 79.1% and 85.6% of their corresponding saturated adsorption capacity, respectively. This may be due to the existence of a large number of effective adsorption sites on the surface of LDHs@PDA-Fe(III) and LDHs@PDA at the initial stage of adsorption, coupled with the large concentration gradient of Cr(VI) on the surface of solution and material at this time. The strong driving force of mass transfer, and the fast diffusion rate, thus leading to the fast adsorption rate [23]. With the further progress of adsorption, the effective adsorption sites on LDHs@PDA-Fe(III) and LDHs@PDA surface are occupied, and the Cr(VI) concentration gradient on the surface of the solution and the material rapidly decreases, leading to the gradual decrease of the adsorption rate until the equilibrium state is reached. The equilibrium time of LDHs@PDA-Fe(III) and LDHs@PDA adsorption of Cr(VI) is 300 min and 420 min, respectively, while the equilibrium adsorption capacity reaches 215.52 mg/g and 123.25 mg/g, respectively. It is suggested that the doping of Fe(III) can not only improve the equilibrium adsorption capacity, but also accelerate the adsorption rate. As displayed in Fig.6, the experimental results are more consistent with the pseudo-second-order kinetic model (R^2=0.9882 and 0.9689). The equilibrium adsorption capacity q_e (220.26 mg/g, 124.65 mg/g) obtained by fitting is closer to the actual equilibrium adsorption capacity q_e (215.52 mg/g, 123.25 mg/g) obtained by experiment. It indicated that the rate control step of the adsorption process was

chemisorption. It is mainly through the chemical reaction between Cr(VI) and LDHs@PDA-Fe(III) and the surface active sites of the bulk material, which indicates that the process is more dependent on the effective adsorption sites on the surface of LDHs@PDA-Fe(III) and LDHs@PDA rather than the residual concentration of Cr(VI) in the solution [42].

Table 1 LDHs@PDA-Fe(III) Kinetic parameters of Cr(VI) adsorption.

Kinetic model	Parameters		
Pseudo-first-order	q_e (mg·g^{-1})	k_1 (min^{-1})	R^2
	202.24	0.0511	0.8895
Pseudo-second-order	q_e (mg·g^{-1})	k_2 (g·mg^{-1}·min^{-1})	R^2
	220.26	3.37×10^{-4}	0.9882

Table 2 LDHs@PDA Kinetic parameters of Cr(VI) adsorption.

Kinetic model	Parameters		
Pseudo-first-order	q_e (mg·g^{-1})	k_1 (mg·g^{-1})	R^2
	117.07	0.0511	0.8061
Pseudo-second-order	q_e (mg·g^{-1})	k_2 (g·mg^{-1}·min^{-1})	R^2
	124.65	8.48×10^{-4}	0.9689

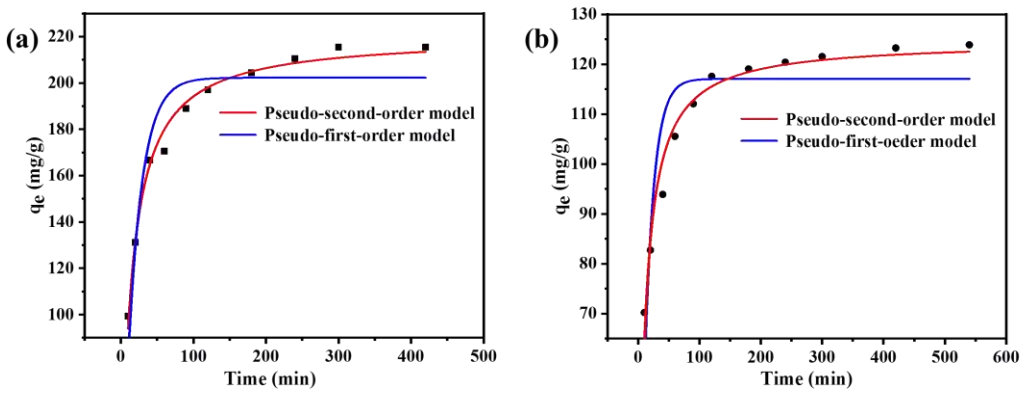

Fig. 6 (a) LDHs@PDA-Fe(III) and (b) LDHs@PDA adsorption of Cr(VI) fitting by pseudo-first-order and pseudo-second-order kinetic models (condition: pH=3, Cr(VI) concentration:100 mg/L, T=298 K).

3.5 Adsorption isotherm and thermodynamics

The adsorption isotherm reflects the relationship between the concentration of adsorbents in solid phase and liquid phase at equilibrium. It is easy to judge the nonlinear adsorption or linear adsorption, and the maximum adsorption capacity of the adsorbent can be obtained by fitting. In order to further explore the isothermal adsorption characteristics of Cr(VI) adsorption process of LDHs@PDA-Fe(III), Langmuir and Freundlich isothermal adsorption models were used to fit the Cr(VI) adsorption process of LDHs@PDA-Fe(III). Relevant equations of isothermal adsorption model are as follows:

Langmuir: $q_e = \frac{q_{\max} K_L C_e}{1 + K_L C_e}$ (4)

Freundlich: $q_e = K_F C_e^n$ (5)

Where q_e, q_{max} are adsorption capacity (mg/g) and maximum adsorption capacity at equilibrium, respectively; K_L (L/g) represents the Langmuir model constant; K_F ($mg^{1-n} \cdot g^{-1} \cdot L^n$) represents Freundlich model constant; n is the adsorption force parameters of Freundlich model. The fitting results and parameters of the isothermal adsorption model are shown in Fig. 7 and Table 3. The adsorption capacity of Cr(VI) at the three temperatures all increased significantly with the increase of the initial concentration of Cr(VI). When C_0=800 mg/L and T=298 K, LDHs@PDA-Fe(III) has an effect on Cr(VI) The adsorption amount reached the experimental maximum of 683.4 mg/g, which may be due to the increase of the concentration gradient of Cr(VI) on the surface of the material and the liquid phase. The mass transfer driving force and diffusion rate of Cr(VI) diffusion to the surface of LDHs@PDA-Fe(III) continue to increase, which in turn causes the adsorption equilibrium state to continue to move in the direction of increasing adsorption capacity.The adsorption process of Cr(VI) in LDHs@PDA-Fe(III) is more consistent with the basic assumption of Freundlich isothermal adsorption model, indicating that the adsorption process of Cr(VI) in LDHs@PDA-Fe(III) is a multi-layer chemical adsorption process. The adsorption capacity increases significantly with the increase of temperature. This implies that the adsorption process of Cr(VI) by LDHs@PDA-Fe(III) is endothermic. In addition, n <1 also indicates that Cr(VI) is favorably adsorbed on the surface of LDHs@PDA-Fe(III) [43].

Table 3 Isothermal parameters of Cr(VI) adsorption.

T (K)	Langmuir			Freundlich		
	q_m (mg/g)	K_L (L/mg)	R^2	n	K_F (L/mg)	R^2
298 K	688.82	0.0278	0.9262	0.2943	113.4992	0.99
303 K	566.69	0.0326	0.9266	0.2709	106.8929	0.9799
308K	422.47	0.0512	0.9725	0.2061	118.2613	0.9612

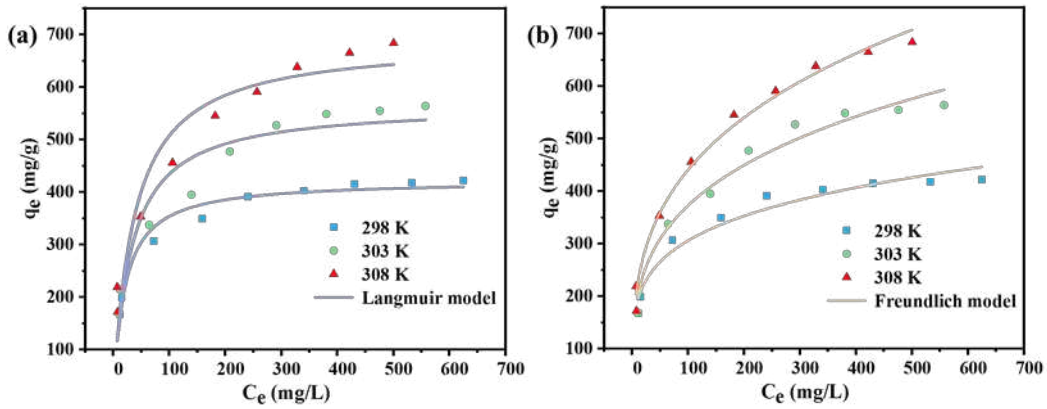

Fig. 7 LDHs@PDA-Fe(III) adsorption experimental data fitting by (a) Langmuir and (b) Freundlich models (condition: pH=3, Cr(VI) concentration: 80-800 mg/L, T=298 K, 303 K and 308 K).

In order to further study the thermodynamic characteristics of Cr(VI) adsorption by LDHs@PDA-Fe(III), the thermodynamic parameters of adsorption (ΔH^0, ΔS^0 and ΔG^0) were calculated from the temperature-dependent adsorption isotherm. The relevant calculation formula is as follows:

$$\Delta G^0 = -RT \ln K^0 \tag{6}$$

$$\ln K^0 = -\frac{\Delta H^0}{RT} + \frac{\Delta S^0}{R} \tag{7}$$

Where R (8.314 $J \cdot mol^{-1} \cdot K^{-1}$) is ideal gas constant; T (K) is temperature; K^0 is standard adsorption equilibrium constant; The fitting and calculated results are shown in Table 4, where ΔH^0 is positive, indicating that the adsorption process of LDHs@PDA-Fe(III) to Cr(VI) is endothermic. A positive value of ΔS^0 indicates that the degree of chaos increases gradually in the process. A negative value of ΔG^0 indicates that the adsorption process is spontaneous. In summary, the adsorption process of LDHs@PDA-Fe(III) to Cr(VI) is a multi-layer chemical adsorption process with spontaneous heat absorption and entropy increase.

Table 4 Thermodynamic parameters of Cr(VI) adsorption.

ΔH^0	ΔS^0	ΔG^0（KJ·mol^{-1}）		
（KJ·mol^{-1}）	（J·mol^{-1}·K^{-1}）	298.15K	303.15K	308.15K
39.48	149.71	-5.196	-5.835	-6.696

3.6 Adsorption mechanism

The XPS analysis results of LDHs@PDA-Fe(III) are shown in Fig. 8, Fig. 8a shows that the main components of LDHs@PDA-Fe(III), such as Mg, Al, C, O, N and Fe are successfully identified, indicating the successful preparation of LDHs@PDA-Fe(III) composite material. A new Cr 2p peak is detected on the surface of LDHs@PDA-Fe(III) after adsorption, indicating that Cr is successfully adsorbed and fixed on the surface of LDHs@PDA-Fe(III). In addition, as shown in Fig. 8b and Fig. 8c, the N 1s spectra changed significantly before and after adsorption. Before adsorption, the peaks at 399.94 eV, 399.61 eV and 398.44 eV correspond to C=N, C-N and N-H, respectively. When the adsorption is in equilibrium, the binding energies of C=N and C-N move to 401.7 eV and 399.86 eV, respectively, while the peak of N-H disappears. It is include that the N-containing functional group strongly interacts with Cr(VI) during the adsorption process [23]. Fig. 8d shows the Cr 2p pattern fixed on the surface of LDHs@PDA-Fe(III) after adsorption, which can be divided into four peaks. The peaks at 586.45 eV and 579.83 eV belong to the Cr $2p_{1/2}$ and Cr $2P_{3/2}$ peaks of Cr(III) [42], respectively. The peaks at 588.79 eV and 576.91 eV belong to the Cr $2P_{1/2}$ and Cr $2p_{3/2}$ peaks of Cr(VI), respectively. The results reveal that part of Cr(VI) is reduced to Cr(III) by catechol in PDA [43]. The catechol in the corresponding PDA would be oxidized to carboxyl group. The O 1s spectrum of LDHs@PDA-Fe(III) after adsorption is shown in Fig. 8e. The peaks of binding energy at 532.71 eV, 531.13 eV and 529.51 eV correspond to H_2O, OH and O-Cr-O [8], respectively. The OH may be related to the $Cr(OH)_3$ deposited on the surface of LDHs@PDA-Fe(III). While O-Cr-O is related to CrO_4^{2-} and $Cr_2O_7^{2-}$. In all, the results of XPS analysis showed that the complexation of functional groups and the reduction of Cr(VI) by PDA played a crucial role in the adsorption process of Cr(VI) by LDHs@PDA-Fe(III).

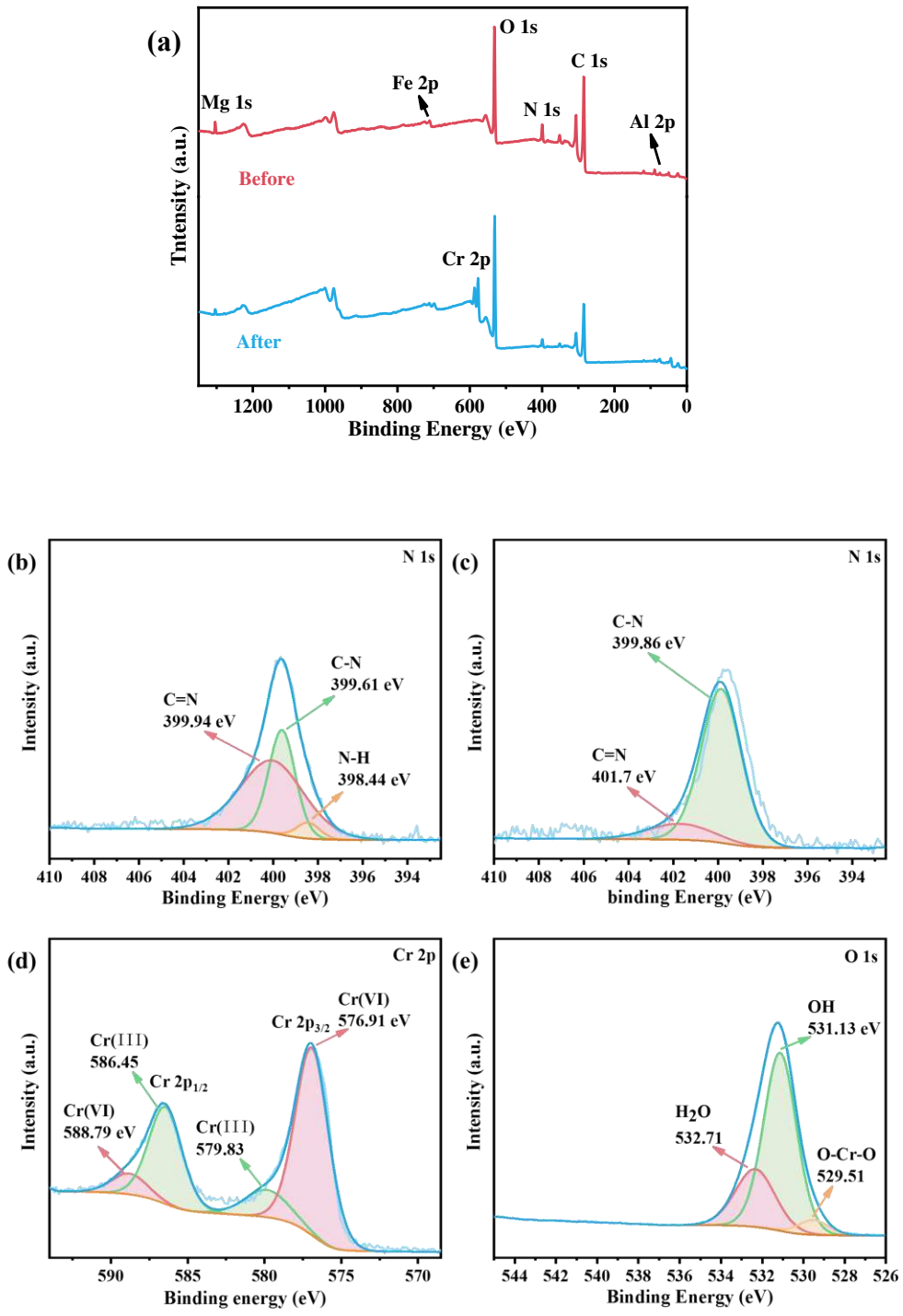

Fig. 8 (a) XPS wide spectra of LDHs@PDA-Fe(III) before and after Cr(VI) adsorption; N 1s spectra of LDHs@PDA-Fe(III) (b) before and (c) after Cr(VI) adsorption; (d) Cr 2p and (e) O 1s spectra of LDHs@PDA-Fe(III) after Cr(VI) adsorption.

3.6 Desorption and regeneration performance

Reusable ability is an important index to evaluate the economy and stability of adsorbents, LDHs@PDA-Fe(III) desorption and resorption results are shown in Fig. 9, with the increase of desorption and resorption cycles, the adsorption capacity of Cr(VI) on LDHs@PDA-Fe(III) decreases somewhat. After 5 regeneration cycles, the adsorption capacity is still 79.3% of the original adsorption capacity. which may be due to the incomplete desorption of Cr(VI) fixed by the material. In addition, the pore structure of the material surface is blocked by Cr(VI) deposits during the adsorption process, which gradually reduces the effective adsorption sites on the surface of LDHs@PDA-Fe(III), resulting in a decline in adsorption performance. In addition, with the continuous oxidation of catechol in PDA to carboxyl group, the reducing power of LDHs@PDA-Fe(III) is also decreased. In short, LDHs@PDA-Fe(III) has good recovery ability and is an ideal material for removing Cr(VI) in wastewater.

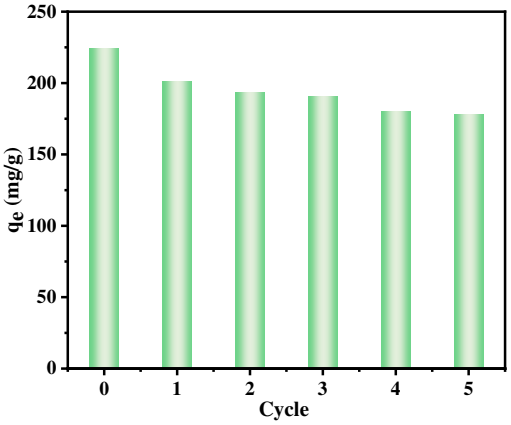

Fig. 9 Effect of regeneration times on LDHs@PDA-Fe(III) adsorption of Cr(VI) (condition: pH=3, Cr(VI) concentration: 100 mg/L, T=298 K).

4. Conclusion

In this study, LDHs@PDA-Fe(III) composite material was prepared and applied to the efficient removal of Cr(VI) in aqueous solution. Notably, LDHs@PDA-Fe(III) showed stronger adsorption efficiency than LDHs@PDA and LDHs, indicating that PDA and Fe(III) were the main binding sites for the capture of Cr(VI) and showed synergistic effects. In addition, based on adsorption data and material characterization

data, the adsorption process can be explained by ion exchange, electrostatic attraction and reduction. In summary, LDHs@PDA-Fe(III) has the advantages of high adsorption capacity, fast adsorption rate, reusability and sufficient stability. It can be used as a potential adsorbent for removing Cr(VI).

Declaration of Competing Interest

The authors declare that they have no known competing financial interests or personal relationships that could have appeared to influence the work reported in this paper.

Acknowledgments

This research did not receive any specific grant from funding agencies in the public, commercial, or not-for-profit sectors.

References

[1] Y. Li, H. Zhu, C. Zhang, M. Cheng, H. He, PEI-grafted magnetic cellulose for Cr(VI) removal from aqueous solution, Cellulose. 25 (2018) 4757–4769. https://doi.org/10.1007/s10570-018-1868-2.

[2] H. Chen, Z. Zhang, X. Zhong, Z. Zhuo, S. Tian, S. Fu, Y. Chen, Y. Liu, Constructing MoS2/Lignin-derived carbon nanocomposites for highly efficient removal of Cr(VI) from aqueous environment, J. Hazard. Mater. 408 (2021) 124847. https://doi.org/10.1016/j.jhazmat.2020.124847.

[3] S. Bao, W. Yang, Y. Wang, Y. Yu, Y. Sun, K. Li, PEI grafted amino-functionalized graphene oxide nanosheets for ultrafast and high selectivity removal of Cr(VI) from aqueous solutions by adsorption combined with reduction: Behaviors and mechanisms, Chem. Eng. J. 399 (2020) 125762. https://doi.org/10.1016/j.cej.2020.125762.

[4] I. Kretschmer, A.M. Senn, J.M. Meichtry, G. Custo, E.B. Halac, R. Dillert, D.W. Bahnemann, M.I. Litter, Photocatalytic reduction of Cr(VI) on hematite nanoparticles in the presence of oxalate and citrate, Appl. Catal. B Environ. 242 (2019) 218–226. https://doi.org/10.1016/j.apcatb.2018.09.059.

[5] S. Bandehali, F. Parvizian, A.R. Moghadassi, S.M. Hosseini, J.N. Shen, Fabrication of thin film-PEI nanofiltration membrane with promoted separation performances: Cr, Pb and Cu ions removal from water, J. Polym. Res. 27 (2020). https://doi.org/10.1007/s10965-020-02056-x.

[6] M. Liang, Y. Ding, Q. Zhang, D. Wang, H. Li, L. Lu, Removal of aqueous Cr(VI) by magnetic biochar derived from bagasse, Sci. Rep. 10 (2020) 1–13. https://doi.org/10.1038/s41598-020-78142-3.

[7] Y. Shi, R. Shan, L. Lu, H. Yuan, H. Jiang, Y. Zhang, Y. Chen, High-efficiency removal of Cr(VI) by modified biochar derived from glue residue, J. Clean. Prod. 254 (2020) 119935. https://doi.org/10.1016/j.jclepro.2019.119935.

[8] K. Zhu, Y. Gao, X. Tan, C. Chen, Polyaniline-Modified Mg/Al Layered Double Hydroxide Composites and Their Application in Efficient Removal of Cr(VI), ACS Sustain. Chem. Eng. 4 (2016) 4361–4369. https://doi.org/10.1021/acssuschemeng.6b00922.

[9] X.Y. Yu, T. Luo, Y. Jia, R.X. Xu, C. Gao, Y.X. Zhang, J.H. Liu, X.J. Huang, Three-dimensional hierarchical flower-like Mg-Al-layered double hydroxides: Highly efficient adsorbents for As(v) and Cr(vi) removal, Nanoscale. 4 (2012) 3466–3474. https://doi.org/10.1039/c2nr30457k.

[10] M. Luo, C. Huang, F. Chen, C. Chen, H. Li, Removal of aqueous Cr(VI) using magnetic-gelatin supported on Brassica-straw biochar, J. Dispers. Sci. Technol. 0 (2020) 1–13. https://doi.org/10.1080/01932691.2020.1785889.

[11] X. Lu, X. Liu, W. Zhang, X. Wang, S. Wang, T. Xia, The residue

from the acidic concentrated lithium bromide treated crop residue as biochar to remove Cr (VI), Bioresour. Technol. (2019) 122348. https://doi.org/10.1016/j.biortech.2019.122348.

[12] J. Guo, J.J. Li, C.C. Wang, Adsorptive removal of Cr(VI) from simulated wastewater in MOF BUC-17 ultrafine powder, J. Environ. Chem. Eng. 7 (2019) 102909. https://doi.org/10.1016/j.jece.2019.102909.

[13] L.L. Li, X.Q. Feng, R.P. Han, S.Q. Zang, G. Yang, Cr(VI) removal via anion exchange on a silver-triazolate MOF, J. Hazard. Mater. 321 (2017) 622–628. https://doi.org/10.1016/j.jhazmat.2016.09.029.

[14] W. Zhang, L. Qian, Y. Chen, D. Ouyang, L. Han, X. Shang, J. Li, M. Gu, M. Chen, Nanoscale zero-valent iron supported by attapulgite produced at different acid modification: Synthesis mechanism and the role of silicon on Cr(VI) removal, Chemosphere. 267 (2021) 129183. https://doi.org/10.1016/j.chemosphere.2020.129183.

[15] K.H. Goh, T.T. Lim, Z. Dong, Application of layered double hydroxides for removal of oxyanions: A review, Water Res. 42 (2008) 1343–1368. https://doi.org/10.1016/j.watres.2007.10.043.

[16] D. Huang, C. Liu, C. Zhang, R. Deng, R. Wang, W. Xue, H. Luo, G. Zeng, Q. Zhang, X. Guo, Cr(VI) removal from aqueous solution using biochar modified with Mg/Al-layered double hydroxide intercalated with ethylenediaminetetraacetic acid, Bioresour. Technol. 276 (2019) 127–132. https://doi.org/10.1016/j.biortech.2018.12.114.

[17] H. Xu, S. Zhu, M. Xia, F. Wang, Rapid and efficient removal of diclofenac sodium from aqueous solution via ternary core-shell CS@PANI@LDH composite: Experimental and adsorption mechanism study, J. Hazard. Mater. 402 (2021) 123815. https://doi.org/10.1016/j.jhazmat.2020.123815.

[18] Q. Wang, Q. Lin, Q. Li, K. Li, L. Wu, S. Li, H. Liu, As(III) removal from wastewater and direct stabilization by in-situ formation of Zn-Fe layered double hydroxides, J. Hazard. Mater. 403 (2021) 123920. https://doi.org/10.1016/j.jhazmat.2020.123920.

[19] P. Zhong, X. Qiu, J. Chen, Removal of bisphenol A using Mg-Al-layer double hydroxide and Mg-Al calined layer double hydroxide, Sep. Sci. Technol. 55 (2020) 501–512. https://doi.org/10.1080/01496395.2019.1577265.

[20] Z. Changani, A. Razmjou, A. Taheri-Kafrani, M.E. Warkiani, M. Asadnia, Surface modification of polypropylene membrane for the removal of iodine using polydopamine chemistry, Chemosphere. 249 (2020) 126079. https://doi.org/10.1016/j.chemosphere.2020.126079.

[21] L.M. Furtado, R.A. Ando, D.F.S. Petri, Polydopamine-coated cellulose acetate butyrate microbeads for caffeine removal, J. Mater. Sci. 55 (2020) 3243–3258. https://doi.org/10.1007/s10853-019-04169-1.

[22] P. Kallem, I. Othman, M. Ouda, S.W. Hasan, I. AlNashef, F. Banat, Polyethersulfone hybrid ultrafiltration membranes fabricated with polydopamine modified ZnFe2O4 nanocomposites: Applications in humic acid removal and oil/water emulsion separation, Process Saf. Environ. Prot. 148 (2021) 813–824. https://doi.org/10.1016/j.psep.2021.02.002.

[23] J. Li, S. Chen, H. Xiao, G. Yao, Y. Gu, Q. Yang, B. Yan, Highly efficient removal of Cr(vi) ions from wastewater by the pomegranate-like magnetic hybrid nano-adsorbent of polydopamine and Fe 3 O 4 nanoparticles , New J. Chem. 44 (2020) 12785–12792. https://doi.org/10.1039/d0nj01293a.

[24] H.C. Yang, Q.Y. Wu, L.S. Wan, Z.K. Xu, Polydopamine gradients by oxygen diffusion controlled autoxidation, Chem. Commun. 49 (2013) 10522–10524. https://doi.org/10.1039/c3cc46127k.

[25] Q. Zhang, Y. Li, Q. Yang, H. Chen, X. Chen, T. Jiao, Q. Peng, Distinguished Cr(VI) capture with rapid and superior capability using polydopamine microsphere: Behavior and mechanism, J. Hazard. Mater. 342 (2018) 732–740. https://doi.org/10.1016/j.jhazmat.2017.08.061.

[26] C. Zhang, Y. Ou, W.X. Lei, L.S. Wan, J. Ji, Z.K. Xu, CuSO4/H2O2-Induced Rapid Deposition of Polydopamine Coatings with High Uniformity and Enhanced Stability, Angew. Chemie - Int. Ed. 55 (2016) 3054–3057. https://doi.org/10.1002/anie.201510724.

[27] L. Zhang, J. Shi, Z. Jiang, Y. Jiang, R. Meng, Y. Zhu, Y. Liang, Y. Zheng, Facile preparation of robust microcapsules by manipulating metal-coordination interaction between biomineral layer and bioadhesive layer, ACS Appl. Mater. Interfaces. 3 (2011) 597–605. https://doi.org/10.1021/am101184h.

[28] D. Zhou, L. Yang, L. Yu, J. Kong, X. Yao, W. Liu, Z. Xu, X. Lu, Fe/N/C hollow nanospheres by Fe(iii)-dopamine complexation-assisted one-pot doping as nonprecious-metal electrocatalysts for oxygen reduction, Nanoscale. 7 (2015) 1501–1509. https://doi.org/10.1039/c4nr06366j.

[29] J.J. Wilker, The iron-fortified adhesive system of marine mussels, Angew. Chemie - Int. Ed. 49 (2010) 8076–8078. https://doi.org/10.1002/anie.201003171.

[30] B. Chen, Y. Cao, H. Zhao, F. Long, X. Feng, J. Li, X. Pan, A novel Fe3+-stabilized magnetic polydopamine composite for enhanced selective adsorption and separation of Methylene blue from complex wastewater, J. Hazard. Mater. 392 (2020) 122263. https://doi.org/10.1016/j.jhazmat.2020.122263.

[31] Z. Yu, X. Zhang, Y. Huang, Magnetic chitosan-iron(III) hydrogel as a fast and reusable adsorbent for chromium(VI) removal, Ind. Eng. Chem. Res. 52 (2013) 11956–11966. https://doi.org/10.1021/ie400781n.

[32] T. Wen, X. Wu, X. Tan, X. Wang, A. Xu, One-pot synthesis of water-swellable Mg-Al layered double hydroxides and graphene oxide

nanocomposites for efficient removal of As(V) from aqueous solutions, ACS Appl. Mater. Interfaces. 5 (2013) 3304–3311. https://doi.org/10.1021/am4003556.

[33] K. Zhu, C. Chen, H. Xu, Y. Gao, X. Tan, A. Alsaedi, T. Hayat, Cr(VI) Reduction and Immobilization by Core-Double-Shell Structured Magnetic Polydopamine@Zeolitic Idazolate Frameworks-8 Microspheres, ACS Sustain. Chem. Eng. 5 (2017) 6795–6802. https://doi.org/10.1021/acssuschemeng.7b01036.

[34] A. Nematollahzadeh, S. Seraj, B. Mirzayi, Catecholamine coated maghemite nanoparticles for the environmental remediation: Hexavalent chromium ions removal, Chem. Eng. J. 277 (2015) 21–29. https://doi.org/10.1016/j.cej.2015.04.135.

[35] J. Zhu, M.T. Tsehaye, J. Wang, A. Uliana, M. Tian, S. Yuan, J. Li, Y. Zhang, A. Volodin, B. Van der Bruggen, A rapid deposition of polydopamine coatings induced by iron (III) chloride/hydrogen peroxide for loose nanofiltration, J. Colloid Interface Sci. 523 (2018) 86–97. https://doi.org/10.1016/j.jcis.2018.03.072.

[36] S. Zhao, Y. Zhan, X. Wan, S. He, X. Yang, J. Hu, G. Zhang, Selective and efficient adsorption of anionic dyes by core/shell magnetic MWCNTs nano-hybrid constructed through facial polydopamine tailored graft polymerization: Insight of adsorption mechanism, kinetic, isotherm and thermodynamic study, J. Mol. Liq. 319 (2020) 114289. https://doi.org/10.1016/j.molliq.2020.114289.

[37] P. Shi, X. Hu, M. Duan, A UIO-66/tannic acid/chitosan/polyethersulfone hybrid membrane-like adsorbent for the dynamic removal of dye and Cr (VI) from water, J. Clean. Prod. 290 (2021) 125794. https://doi.org/10.1016/j.jclepro.2021.125794.

[38] P. Liu, X. Wang, J. Ma, H. Liu, P. Ning, Highly efficient immobilization of NZVI onto bio-inspired reagents functionalized polyacrylonitrile membrane for Cr(VI) reduction, Chemosphere. 220 (2019) 1003–1013. https://doi.org/10.1016/j.chemosphere.2018.12.163.

[39] J. Matusik, J. Hyla, P. Maziarz, K. Rybka, T. Leiviskä, Performance of halloysite-Mg/Al LDH materials for aqueous as(V) and Cr(VI) removal, Materials (Basel). 12 (2019) 1–16. https://doi.org/10.3390/ma12213569.

[40] Y. Zhang, M. Li, J. Li, Y. Yang, X. Liu, Surface modified leaves with high efficiency for the removal of aqueous Cr (VI), Appl. Surf. Sci. 484 (2019) 189–196. https://doi.org/10.1016/j.apsusc.2019.04.088.

[41] L. Ma, X. Shi, X. Zhang, S. Dong, L. Li, Electrospun Cellulose Acetate–Polycaprolactone/Chitosan Core–Shell Nanofibers for the Removal of Cr(VI), Phys. Status Solidi Appl. Mater. Sci. 216 (2019) 1–9. https://doi.org/10.1002/pssa.201900379.

[42] H.W. Kwak, H. Lee, K.H. Lee, Surface-modified spherical lignin

particles with superior Cr(VI) removal efficiency, Chemosphere. 239 (2020) 124733. https://doi.org/10.1016/j.chemosphere.2019.124733.

[43] L. Dong, R. Deng, H. Xiao, F. Chen, Y. Zhou, J. Li, S. Chen, B. Yan, Hierarchical polydopamine coated cellulose nanocrystal microstructures as efficient nanoadsorbents for removal of Cr(VI) ions, Cellulose. 26 (2019) 6401–6414. https://doi.org/10.1007/s10570-019-02529-3.